Plant Physiology and Biochemistry 223 (2025) 109875

Contents lists available at ScienceDirect

Plant Physiology and Biochemistry

journal homepage: www.elsevier.com/locate/plaphy

A naturally integrated *RolD-like* gene in sweet potato mediates stress-responsive pathways

Yulia Yugay, Tatiana Rusapetova, Elena Vasyutkina, Maria Sorokina, Valeria Grigorchuk, Veronika Degtyareva, Dina Rudenko, Egor Alaverdov, Victor Bulgakov, Yury Shkryl *

Federal Scientific Center of the East Asia Terrestrial Biodiversity of the Far East Branch of Russian Academy of Sciences, Vladivostok, 690022, Russia

ARTICLE INFO

Keywords:
Agrobacterium rhizogenes
Ipomoea batatas
Naturally transgenic plants
rol genes
T-DNA

ABSTRACT

Sweet potato (*Ipomoea batatas*), a globally significant staple crop, exhibits remarkable adaptability to various environmental conditions, largely due to its genetic diversity. Recent studies have revealed the presence of naturally integrated *Agrobacterium* cellular T-DNAs (cT-DNAs) within the sweet potato genome, suggesting their possible role in the evolution and adaptation of sweet potato. In this study, we characterize a newly identified open reading frame (ORF) within the cT-DNA2 region of *I. batatas*, which encodes a homolog of the *A. rhizogenes rolD* gene. This ORF encodes a RolD-like protein with ornithine cyclodeaminase (OCD) activity, a key enzyme in proline biosynthesis. Functional assays confirmed that the recombinant RolD-like protein exhibits ornithine-dependent NAD^+ reduction, similar to the product of the *rolD* gene. Notably, *rolD-like* gene expression was strongly up-regulated by methyl jasmonate treatment, as well as in response to abiotic stresses such as heat, cold, salt, drought, high light, and UV radiation. Overexpression of this *rolD-like* gene in *Arabidopsis thaliana* resulted in delayed flowering, shortened siliques, and reduced seed production, along with enhanced proline accumulation, indicating its role in stress response mechanisms. These findings suggest that the natural integration of this *rolD-like* gene may contribute to the sweet potato's resilience to abiotic stresses, offering potential for the development of improved cultivars with enhanced stress tolerance.

1. Introduction

Sweet potato (*Ipomoea batatas*) is recognized as one of the most significant food crops globally, ranking as the seventh most important staple after rice, wheat, and maize (Sapakhova et al., 2023). This prominence is attributed to its rich nutritional profile, which includes essential vitamins, minerals, and dietary fiber, making it a vital source of energy and nutrition, particularly in developing countries (Kays, 2005). Beyond its nutritional value, sweet potato exhibits remarkable adaptability to a wide range of environmental conditions, allowing it to thrive across diverse agro-ecological zones in Asia, Africa, and Latin America (Motsa et al., 2015). This adaptability, coupled with its resilience to abiotic stresses such as drought, is becoming increasingly crucial in the context of climate change.

The genetic diversity of sweet potato play a critical role in its adaptability and yield stability (Rodriguez-Bonilla et al., 2014; Yan et al., 2022). Ongoing genetic improvement efforts are focused on enhancing traits such as drought tolerance and disease resistance, which are vital for sustaining crop productivity under changing environmental conditions (Laurie et al., 2022). Furthermore, the cultivation of sweet potato is integral to food security and the livelihoods of smallholder farmers who rely on this crop as a staple food source (Mukhopadhyay et al., 2011). Given these factors, understanding the genetic and physiological mechanisms that underpin sweet potato's adaptability and nutritional value is essential for optimizing its cultivation and enhancing global food security (Kwak, 2019).

An intriguing aspect of sweet potato genetics is the phenomenon of natural transgenesis, wherein genes from other species have been naturally integrated into its genome. This is exemplified by the presence of naturally occurring *Agrobacterium* cellular (c)T-DNAs within the sweet potato genome (Kyndt et al., 2015). Studies have identified two independent cT-DNA copies in the cultivated sweet potato genome, each containing open reading frames (ORFs) homologous to genes from *Agrobacterium* species (Kyndt et al., 2015; Quispe-Huamanquispe et al.,

* Corresponding author:Federal Scientific Center of the East Asia Terrestrial Biodiversity of the Far East Branch of Russian Academy of Sciences, 159 Stoletija Str., Vladivostok, 690022, Russia
E-mail address: yn80@mail.ru (Y. Shkryl).

https://doi.org/10.1016/j.plaphy.2025.109875
Received 22 December 2024; Received in revised form 21 February 2025; Accepted 1 April 2025
Available online 1 April 2025

2019). The presence of specific ORFs associated with stress response pathways suggests that these naturally integrated genes may contribute to the plant's ability to respond to environmental stress signals (Vasyutkina et al., 2022). This natural integration not only enhances the plant's adaptability but also raises critical questions about food safety and consumer perceptions of genetically modified organisms.

Recent studies have identified a new ORF encoding a hypothetical protein with a "NADB Rossman" domain located adjacent to the 3′-part of cT-DNA2 (Quispe-Huamanquispe et al., 2019). This ORF is of particular interest because it appears to encode a protein with homology to the *rolD* gene from *A. rhizogenes*, which plays a crucial role in proline metabolism. Ornithine cyclodeaminase (OCD), the enzyme encoded by *rolD*, is pivotal in proline biosynthesis, particularly under stress conditions (Trovato et al., 2018). Proline accumulation is a common response in plants exposed to various abiotic stresses, playing a crucial role in stress tolerance (Hayat et al., 2012). This amino acid functions as an osmolyte, metal chelator, antioxidant, and signaling molecule (Szabados and Savouré, 2010). In sweet potato, proline accumulation serves multiple protective functions, including osmoregulation, stabilization of proteins and membranes, and scavenging of reactive oxygen species (ROS) generated during stress conditions (Imbo et al., 2016).

In this study, we aimed to characterize this novel ORF from *Ib*T-DNA2 and investigate its functional activity. We found that it encodes a RolD-like protein, with confirmed OCD activity, facilitating ornithine-dependent NAD^+ reduction. The transcription of this gene was significantly upregulated under abiotic stress conditions, including heat, cold, salinity, and UV radiation, as well as in response to methyl jasmonate treatment. Overexpression of this *rolD-like* gene in *Arabidopsis thaliana* caused delayed flowering, altered silique morphology, and enhanced proline accumulation, indicating its potential role in stress response mechanisms.

2. Materials and methods

2.1. Sequence verification and structural predictions

To confirm the 3′-end sequence of *Ib*T-DNA2, we performed PCR using sweet potato genomic DNA and gene-specific primers. The forward primer, newORF-D (5′-GAA GAC CTC ACC TCC G-3′), was designed to target the coding sequence (CDS) of a hypothetical protein containing a "NADB Rossmann" domain. The reverse primer, UcpB-D (5′-GAA GGC CTA TAT CTA CAT CTC-3′), was aligned with the sixth exon of the *I. batatas UcpB* gene (GenBank Acc. No. MN159301). PCR amplification produced a 1410-bp fragment, which was subsequently purified and sequenced using an ABI 3500 Genetic Analyzer (Applied Biosystems, Foster City, CA, USA). Sequence analysis using BLAST revealed a high degree of similarity to the *rolD* gene from *A. rhizogenes*. Consequently, this newly identified ORF was designated as "*rolD-like*."

Structural features of *A. tumefaciens* ornithine cyclodeaminase (OCD), RolD from *A. rhizogenes*, and the RolD-like homolog from *I. batatas* were predicted using the PHYRE2 automatic fold recognition server (Kelley et al., 2015). For promoter analysis, a 499-bp upstream sequence of the *rolD-like* gene (GenBank Acc. No. KM052617; 10, 778–11276 bp) was extracted and analyzed using the PlantCARE tool (Lescot et al., 2002) to identify potential cis-regulatory elements.

2.2. Experiments with sweet potato leaves

Changes in *rolD-like* mRNA levels were analyzed using a detached-leaf assay, with the third fully developed leaves selected as described previously (Shkryl et al., 2024). Detached leaves were weighed and placed in Petri dishes containing deionized water, and control leaves were incubated in a growth chamber (KS-200 SPU, Smolensk, Russia) at 23 °C under long-day (LD) conditions with a photosynthetic photon flux density (PPFD) of either 35 or 150 μmol m^{-2} s^{-1} under a 16-h light/8-h dark photoperiod. Young, not fully expanded leaves and old leaves with visible signs of senescence were included in the analysis. To impose darkness stress, attached leaves were covered with aluminum foil for 6 days. Exogenous hormone treatments were applied by treating leaves with 1 mg/L of indole-3-acetic acid (IAA) and kinetin, or 50 μM of abscisic acid (ABA), methyl jasmonate (MeJA), or salicylic acid (SA). Salinity, osmotic, and oxidative stresses were simulated by supplementing the medium with 92 mM NaCl, 153 mM mannitol, or 10 μM paraquat, respectively. Drought stress was induced by placing detached leaves in Petri dishes without added water, while temperature stress was applied by exposing samples to either +6 °C or +47 °C. To evaluate the effects of proline and ornithine on *rolD-like* expression, leaves were treated with 10 mM of each compound. For each treatment described above, the Petri dishes were incubated in a controlled growth chamber for 3 h or 2 days, depending on the experimental protocol. Ultraviolet (UV-C) light stress was induced by exposing leaves to 254 nm UV light for 60 min using a UV lamp (R-52G, UVP Inc., USA) positioned 10 cm from the samples. Intense light stress was induced by exposing leaves to a photosynthetic photon flux density of 1200 μmol/m^2/s for 3 h, with the light source positioned 55 cm from the Petri dishes. All experiments were conducted in triplicate, with four individual leaves sampled for analysis per treatment. Following the experiments, the leaves were frozen in liquid nitrogen and utilized for RNA isolation.

2.3. Gene cloning and binary vector construction

To amplify the full-length sequence of the ***rolD-like*** gene, PCR reactions were performed as described previously (Shkryl et al., 2021), using gene-specific primers: forward primer **rolD-like-D** (5′-ATA GCC ATG GCA GCC AAA ATA TTT TGC-3′) and reverse primer **rolD-like-R** (5′-GAC TCT AGA CCT AGA GGG CAC CAA TGA-3′). The amplified sequence was sub-cloned as an ***Nco*I-*Xba*I** fragment into the corresponding sites of the linearized **pSAT6-MCS** vector, placing the gene under the control of the 35 S CaMV promoter and terminator. The resulting construct was confirmed by DNA sequencing, which verified the absence of mutations. Subsequently, the expression cassette was excised as a **PI-*Psp*I** fragment and sub-cloned into the same site of the binary vector **pPZP-RCS2-Ocs:nptII**, which carries the neomycin phosphotransferase gene (**nptII**) for kanamycin selection under the control of the octopine synthase (**Ocs**) promoter and terminator (Shkryl et al., 2024). The final construct, **pPZP-RCS2-Ocs:nptII/35S:rolD-like**, was introduced into ***Agrobacterium tumefaciens*** strain **EHA105/p-TiBo542** via the GenePulser Xcell™ electroporation system (Bio-Rad Laboratories, Inc., Hercules, CA, USA), following the manufacturer's protocol.

2.4. Hairy roots induction test

The ability of *A. tumefaciens* strain EHA105 carrying the pPZP-RCS2-Ocs:nptII/35 S:rolD-like construct, either alone or in combination with *A. rhizogenes* strain K599, to induce hairy root syndrome was evaluated. Empty *A. tumefaciens* EHA105 (without the binary vector) served as the negative control, while wild-type *A. rhizogenes* K599 was used as the positive control. Preparation of *Agrobacterium* strains for transformation followed previously described protocols (Shkryl et al., 2024). Internodes of *Kalanchoë daigremontiana* plants grown in soil were wounded and directly inoculated with the *Agrobacterium* strains using sterile syringes containing bacterial suspensions. Inoculated plants were incubated at 26 °C in a KS-200 climatic test chamber (Smolensk SKTB SPU, Russia) under a 16-h light/8-h dark photoperiod for 30 days to allow for root induction. The hairy root induction experiments were performed in triplicate to ensure reproducibility.

2.5. Obtaining transgenic plants

Wild-type *Arabidopsis thaliana* (Columbia-0) seeds were stratified for 2 days at 4 °C in complete darkness. Stratified seeds were germinated on

half-strength Murashige and Skoog (MS) medium supplemented with 10 g/L sucrose and 8 g/L agar. Germination occurred under a 16-h light/8-h dark photoperiod at 25 °C in a growth chamber. After 10 days, seedlings were transplanted to soil for further development. The pPZP-RCS2-Ocs:nptII/35 S:rolD-like construct was introduced into *A. thaliana* using the floral dip method as described (Shkryl et al., 2021). T1 plants were selected on half-strength MS medium containing 50 mg/L kanamycin, and antibiotic-resistant lines were transplanted to soil to generate homozygous transgenic plants. These lines were confirmed to exhibit no segregation under kanamycin selection. Two independent transgenic lines, designated At-rolD-like1 and At-rolD-like2, were selected for further study. Homozygous T3 transgenic plants were used in all experiments, and growth conditions were identical to those of wild-type plants.

2.6. Isolation of cDNA and real-time PCR analysis

Total RNA isolation and first-strand cDNA synthesis were performed as previously described (Shkryl et al., 2021). For *I. batatas*, various plant parts, including leaf, stem, fibrous roots, shoot apex, and storage root, as well as detached leaves, were analyzed for *rolD-like* mRNA levels. RNA from 5-week-old transgenic *A. thaliana* plants was used for gene expression analysis. Three biological replicates were generated from independent RNA extractions, with each biological replicate analyzed in triplicate for technical replication.

Quantitative real-time PCR (qPCR) was conducted using the Bio-Rad CFX96 Real-Time System (Bio-Rad Laboratories, Hercules, CA, USA) and 2x BioMaster RT-PCR SYBR Blue (Biolabmix®, Novosibirsk, Russia), following previously described protocols (Shkryl et al., 2021). Gene-specific primers used in the qPCR are listed in Supplementary Table 1. *UBI* and *GAPDH* genes were utilized as reference genes for *I. batatas* and *A. thaliana*, respectively. Data analysis was carried out using CFX Manager Software (Version 3.1; Bio-Rad Laboratories).

2.7. Protein expression and purification

A bacterial expression system was employed to produce and analyze recombinant proteins. The *rolD-like* gene sequence was amplified using the primers pET-rolD-like-D (5′-TAC CAT GGC GAC GGA AAT TCT TTC-3′) and pET-rolD-like-R (5′-TAG CGG CCG CGG ATC TAG AAT CTA GGA-3′). As a control, the *rolD* gene from *A. rhizogenes* A4 was amplified using the primer pair pET-rolD-D (5′-TAC CAT GGC CAA ACA ACT TTG CGA-3′) and pET-rolD-R (5′-TAG CGG CCG CAT GCC CGT GTT CCA TCG-3′). The resulting PCR products were cloned into the pET40 vector as *Nco*I-*Not*I fragments, and all constructs were verified by sequencing.

For protein expression, *E. coli* BL21 (DE3)pLysS or Rosetta 2 (DE3) strains were transformed with recombinant pET 22 plasmids encoding the *rolD-like* or *rolD* genes using the heat-shock method. Transformed cells were plated on LB agar containing 34 μg/mL chloramphenicol and 50 μg/mL kanamycin. PCR screening with standard T7-promoter and T7-terminator primers verified positive colonies, which were subsequently inoculated into liquid LB media supplemented with the same antibiotics.

Starter cultures grown overnight were diluted 1:50 into fresh MX medium (10 g bacto-tryptone, 2.31 g KH_2PO_4, 12.54 g K_2HPO_4, 0.94 g $MgCl_2$, 4 mL glycerol, 72 g sorbitol, and 7.5 g yeast extract per liter) and incubated at 37 °C with constant shaking at 200 rpm until the OD_{600} reached 1.0 ± 0.1. Following this, cells were cooled to room temperature (~20 °C), and protein expression was induced with isopropyl-β-D-thiogalactopyranoside (IPTG) at a final concentration of 0.2 mM. Induction was carried out at 16 °C for 18 h.

2.8. Preparation of bacterial and plant extracts

Bacterial cells were resuspended in 20 mM potassium phosphate buffer (pH 8.5) at a ratio of 1:5 (w/v). The buffer contained 10 % (v/v) glycerol, 200 mM NaCl, 10 mM dithiothreitol (DTT), 1 mM phenylmethylsulfonyl fluoride (PMSF), 1 mM EDTA disodium salt (pH 8.0), 0.5 mg/mL lysozyme, and 5 U/mL DNAse I. Resuspended cells were sonicated to disrupt the cell membrane and then centrifuged at 18,000×*g* for 30 min. The resulting supernatants, representing soluble protein extracts, were analyzed via SDS-PAGE. Protein concentrations were quantified using the Bradford protein assay (Bio-Rad Laboratories) with bovine serum albumin (BSA) as the standard.

Leaves of 1.5-month-old *A. thaliana* plants were harvested, flash-frozen in liquid nitrogen, and ground into a fine powder. The homogenized plant material was resuspended in cold extraction buffer at a 1:2 (v/v) ratio. The extraction buffer consisted of 20 mM potassium phosphate buffer (pH 8.5), 10 % glycerol, 200 mM NaCl, 10 mM DTT, 1 mM PMSF, and 1 mM EDTA. Samples were centrifuged at 14,000×*g* for 30 min at +4 °C. The supernatants were collected as the plant protein extracts, and protein concentrations were measured using the Bradford protein assay.

2.9. Ornithine cyclodeaminase activity assay

Ornithine cyclodeaminase (OCD) activity was measured following the method described by Trovato et al. (2001) with minor modifications. The reaction mixture consisted of 20 mM potassium phosphate buffer (pH 8.5), 1 mM EDTA disodium salt (pH 8.0), 2 mM NAD+, 10 mM dithiothreitol (DTT), and 1 mM ornithine, which was added immediately before starting the reaction. Each well of a 96-well plate contained 200 μL of the reaction mixture, supplemented with either 150 μg of soluble bacterial protein or 400 μg of total plant protein extract. The accumulation of NADH during the reaction was monitored spectrophotometrically at 340 nm and 37 °C for 4 h. NADH concentrations were calculated using the Beer–Lambert law, employing the molar extinction coefficient for NADH (6.22 L/mmol/cm at 340 nm).

2.10. Proline measurement

Proline content was quantified using an Agilent 1260 Infinity analytical HPLC system (Agilent Technologies, Santa Clara, CA, USA) coupled with a Bruker HCT Ultra PTM ion trap mass spectrometer (Bruker Daltonik GmbH, Bremen, Germany). Hydrophilic interaction chromatography (HILIC) was conducted on a normal-phase Ascentis Si column (Supelco, Bellefonte, PA, USA; 250 × 2.1 mm, 5 μm) maintained at 30 °C. The mobile phase consisted of solution A (15 mM ammonium formate in 0.1 % formic acid) and solution B (acetonitrile). Gradient elution was performed at a flow rate of 0.2 mL/min, with a linear gradient from 60 % to 20 % solution B over 30 min. Positive ion electrospray ionization (ESI) mode was used for detection, with the following instrument settings: mass detection range of *m/z* 50–400, drying gas (N_2) flow rate of 8.0 L/min, nebulizer gas pressure of 25 psi, drying gas temperature of 325 °C, and ion source potential of 4.0 kV. Extracted ion chromatograms for proline were recorded at m/z 116 ± 1 ($[M+H]^+$), and tandem mass spectra for precursor ions at *m/z* 116 were acquired in Auto-MS2 mode to confirm proline identification. L-proline (Sigma–Aldrich Co., St. Louis, MO, USA) was used as an external standard for quantification.

2.11. Quantification of flavonol glycosides

2.11.1. Chemicals

Analytical standards of kaempferol and quercetin were procured from Sigma-Aldrich (St. Louis, MO, USA). Ultra-pure water (Millipore, Bedford, MA, USA) was used to prepare all extraction solutions and eluents. All solvents used were of analytical grade.

2.11.2. Sample preparation

Sample preparation for HPLC-UV analysis followed the protocol described in our previous study (Shkryl et al., 2021). Briefly, dried and

powdered plant tissue was sonicated in 70 % methanol, and the resulting supernatant was filtered through a 0.45-μm membrane (Millipore, Bedford, MA, USA) for subsequent analysis.

2.11.3. Analytical chromatography

Flavonoid quantification was conducted using reversed-phase high-performance liquid chromatography (RP-HPLC) with UV detection. The analysis utilized an Agilent 1260 Infinity HPLC system (Agilent Technologies, Santa Clara, CA, USA) equipped with a Zorbax C18 analytical column (150 mm × 2.1 mm i. d., 3.5-μm particle size, Agilent Technologies, USA) maintained at 40 °C. The mobile phase for gradient elution comprised 0.1 % aqueous formic acid (A) and acetonitrile (B), with a linear gradient elution profile increasing from 0 % to 50 % B over 50 min at a flow rate of 0.2 mL/min. UV spectra were recorded using a diode array detector (DAD) over a wavelength range of 200–600 nm, while chromatograms for quantification were obtained at 265 nm. Flavonoid compounds were quantified using the external standard method, with all flavonol glycosides identified previously in our earlier work (Shkryl et al., 2021).

2.12. Statistical analysis

All data are presented as the mean ± SE. Statistical comparisons between two independent groups were performed using the Student's *t*-test. For comparisons involving multiple groups, analysis of variance (ANOVA) followed by a multiple comparison procedure was employed. Inter-group differences were analyzed using Fisher's protected least significant difference (PLSD) *post-hoc* test. Statistical significance was

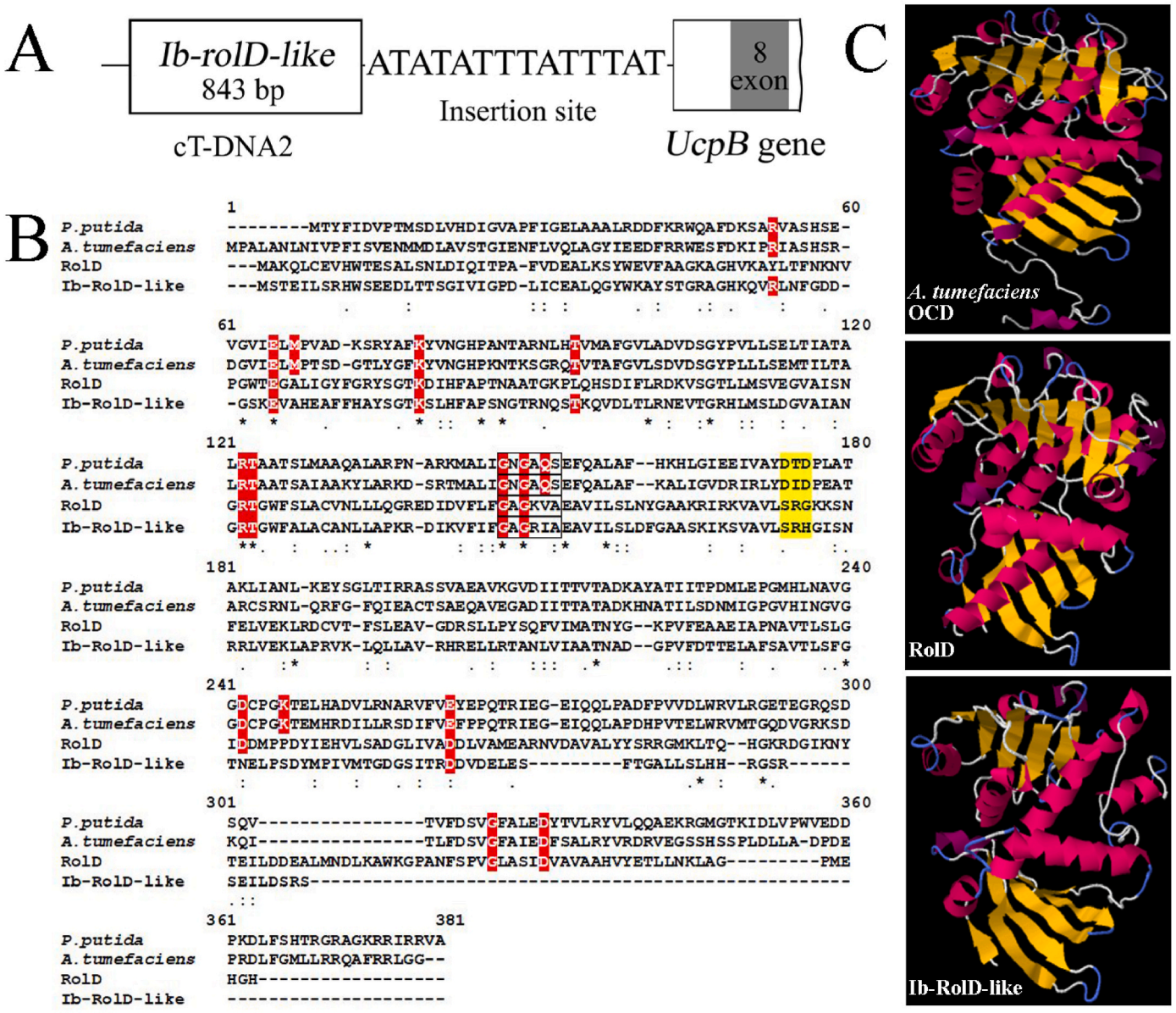

Fig. 1. Characterization of the *rolD-like* gene and protein. (A) Schematic representation of the right end of the *I. batatas* cellular T-DNA2 region, highlighting the *rolD-like* gene and the AT-rich insertion site within the *UcpB* gene. (B) Alignment of deduced amino acid sequences of the RolD-like protein with ornithine cyclodeaminase (OCD) proteins from *P. putida*, *A. tumefaciens*, and the RolD protein from *A. rhizogenes*. Conserved residues in the active site are highlighted in red. The residues that determine cofactor preference are highlighted in yellow. The P-loop sequence is in a frame. Regions of identity (*), conservation, and similarity (.) are indicated below the alignment. GeneBank Accession Numbers: *Pseudomonas putida* OCD (WP010954390), *Agrobacterium tumefaciens* C58 OCD (ASK45285), *A. rhizogenes* RolD (WP_034,521,016), *I. batatas* RolD-like (PQ369418). (C) Predicted 3D structures of OCD from *A. tumefaciens*, RolD from *A. rhizogenes*, and the RolD-like protein from *I. batatas*, illustrating structural similarities. (For interpretation of the references to color in this figure legend, the reader is referred to the Web version of this article.)

defined as $p \leq 0.05$.

3. Results

3.1. Identification and characterization of a rolD-like gene from IbT-DNA2

The *Ib*T-DNA2 (GenBank Acc. No. KM052617) region, previously characterized, comprises five *Agrobacterium* open reading frames (ORFs): ORF14, ORF17n, RolB/RolC, ORF13, and ORF18/17n (Kyndt et al., 2015). A novel ORF containing a "NADB Rossmann" domain was identified at the right end of *Ib*T-DNA2 (Quispe-Huamanquispe et al., 2019). In the original GenBank sequence, this ORF appeared truncated, spanning only 390 bp, and encoding a short protein of 129 amino acids. Given the previous estimation of the *Ib*T-DNA2 insertion locus (Quispe-Huamanquispe et al., 2019), we sought to re-examine its 3′-end sequence to confirm the completeness of this ORF.

Our analysis revealed that the complete ORF consists of an 843 bp coding sequence (CDS), followed by a short AT-rich T-DNA insertion site (GenBank Acc. No. PQ369418), and is flanked by the *UcpB* gene intron (Fig. 1A). The deduced amino acid sequence of this ORF shows strong homology to the *rolD* gene from *A. rhizogenes*, as determined using BLAST, and is hereafter referred to as the ***rolD-like* gene**. Additionally, the RolD-like protein shares significant sequence similarity with ornithine cyclodeaminases (OCDs) from other organisms (Fig. 1B).

The RolD-like protein retains critical conserved residues essential for OCD substrate recognition (Goodman et al., 2004; Mahesh et al., 2022). Similar to the RolD protein, not all catalytic amino acids in the RolD-like protein align with the canonical OCD sequence. However, other characteristic amino acids absent in RolD are present in the RolD-like protein and correspond to those found in bacterial OCDs. The sequence also harbors a P-loop or Rossmann NAD(P)-binding domain (GxGxxG/A/S) followed by a three-residue motif critical for cofactor preference (Fig. 1B). Sequence-based prediction of cofactor specificity for the Rossmann fold in the RolD-like protein was performed using the online tool Cofactory - 1.0 (Geertz-Hansen et al., 2014). The analysis revealed a high specificity for NAD cofactors, consistent with the preferences observed in OCD enzymes from *Pseudomonas putida* and *A. tumefaciens*.

Theoretical modeling of the spatial structure of the RolD-like protein, performed using the PHYRE2 modeling server, revealed structural similarities with both the RolD protein from *A. rhizogenes* and the OCD protein from *A. tumefaciens* (Fig. 1C). These findings suggest that the *rolD-like* gene may encode a functional OCD enzyme with potential implications in proline biosynthesis and stress response.

3.2. Expression and functional analysis of RolD-like proteins in E. Coli

Prior research established that the RolD protein from *A. rhizogenes* exhibits OCD activity (Trovato et al., 2001). Based on these findings, we hypothesized that the RolD-like protein might possess similar enzymatic functions. To test this hypothesis, the full-length sequence of the *rolD-like* gene was cloned into the pET40 vector and expressed in the *E. coli* BL21 (DE3)pLysS strain. For comparison, the full-length *rolD* gene from the *A. rhizogenes* A4 strain was also expressed under the same conditions. Both recombinant proteins were successfully expressed in the soluble fraction, as confirmed by SDS-PAGE analysis (Fig. 2A).

The OCD enzyme catalyzes the direct conversion of L-ornithine to L-proline, with the reaction generating NADH as a byproduct (Goodman et al., 2004; Trovato et al., 2001). To evaluate the OCD activity of the RolD-like protein, we conducted an *in vitro* enzymatic assay. The results confirmed that both RolD and RolD-like proteins catalyzed the conversion of L-ornithine to L-proline. NADH accumulation, which indicates enzymatic activity, was detected spectrophotometrically at 340 nm. A significant increase in NADH concentration was observed, confirming the enzymatic activity of the RolD-like protein (Fig. 2B). These results provide strong evidence that the RolD-like protein exhibits OCD activity, comparable to the well-characterized RolD protein from *A. rhizogenes*.

3.3. Analysis of cis-regulatory motifs and expression profiles of the rolD-like gene

To investigate the regulatory mechanisms underlying the expression of the *rolD-like* gene, we conducted an *in silico* analysis of its 500-bp promoter region to identify cis-regulatory elements potentially involved in transcriptional control and responsiveness to environmental and hormonal signals (Fig. 3A). Within this promoter region, several *cis*-elements were identified, including DRE1 and LTR motifs, which are key regulators of gene expression in response to abiotic stresses such as low temperature, dehydration, and salinity (Yamaguchi-Shinozaki and Shinozaki, 2005). Additionally, conserved light-responsive modules, such as the G-box and Box-4, were detected. These elements are known to mediate transcriptional responses to light signals, thereby influencing

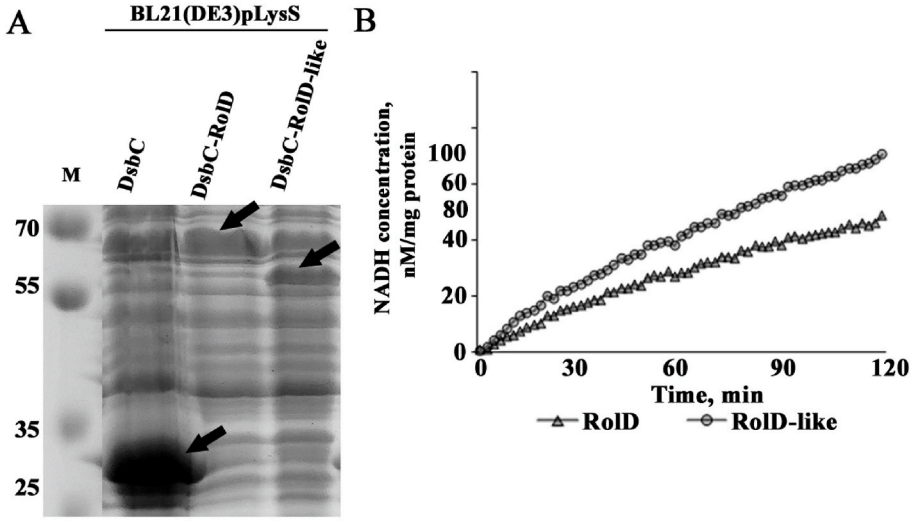

Fig. 2. Enzymatic activity of the RolD-like protein. (A) SDS-PAGE analysis of recombinant DsbC-RolD and DsbC-RolD-like protein expression in *E. coli* BL21 (DE3) pLysS strain. Protein expression was induced with 0.2 mM IPTG and carried out for 18 h at 16 °C. Each lane contains 20 μg of total cell lysate. Lane M represents molecular weight markers (in kDa). Arrows indicate the proteins of interest at their predicted molecular weights. (B) NADH accumulation during the enzymatic conversion of ornithine to proline catalyzed by ornithine cyclodeaminase (OCD). NADH production was monitored spectrophotometrically at 340 nm.

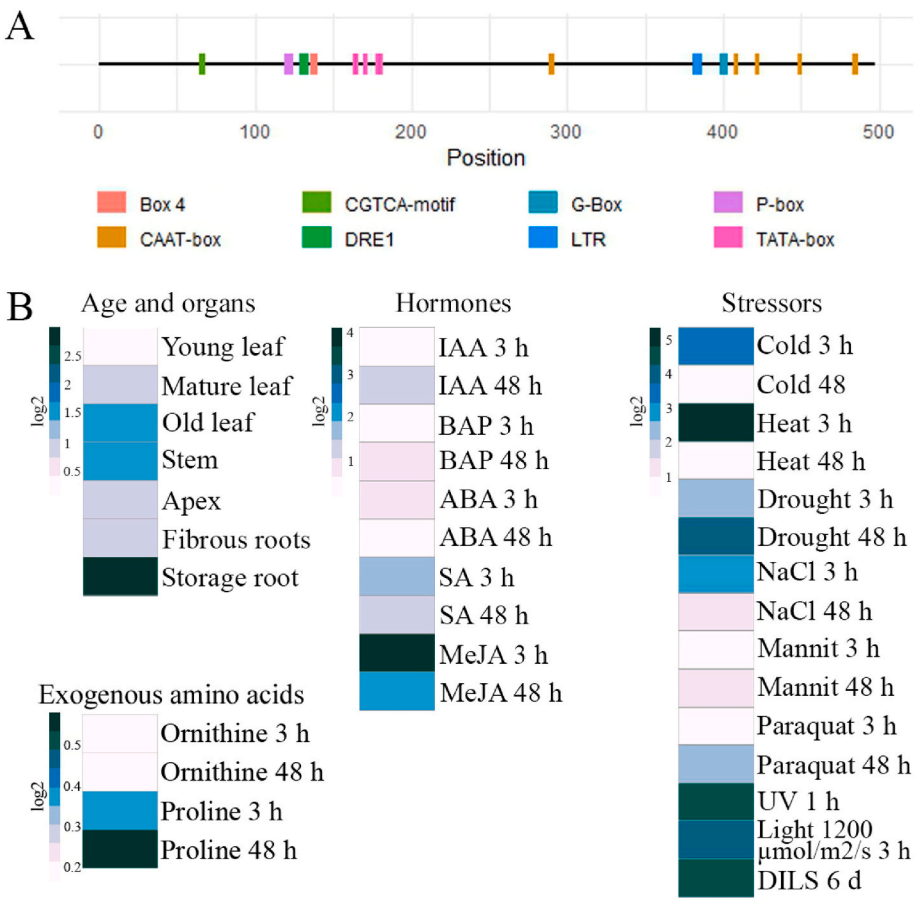

Fig. 3. Cis-element prediction and expression profiles of the ***rolD-like*** gene. (A) Predicted cis-element analysis in the promoter region of the *rolD-like*. The promoter sequence was analyzed using PlantCARE, revealing the presence of various cis-elements represented by color-coded boxes, each corresponding to a specific regulatory motif. (B) Heat map of *rolD-like* gene expression levels across different tissues, in response to hormonal treatments, stress conditions, and exogenous amino acids. Expression data are presented in log 2 scale. (For interpretation of the references to color in this figure legend, the reader is referred to the Web version of this article.)

genes involved in light-regulated processes (Niu et al., 2018; Yin et al., 2013). The G-box, in particular, functions as a molecular switch activated through calcium-dependent phosphorylation or dephosphorylation in response to light. It also provides a binding site for bZIP proteins and is regulated by environmental stimuli such as UV radiation, abscisic acid (ABA), red light, and mechanical injury (Ma et al., 2013).

Furthermore, hormonal regulatory elements such as the CGTCA motif and P-box were identified (Fig. 3A). The CGTCA motif serves as a binding site for transcription factors involved in methyl jasmonate signaling (Rouster et al., 1997), while the P-box element plays a role in regulating the remobilization of storage compounds during seed germination under the influence of gibberellic acid (Schmidt et al., 2014). Finally, the promoter contains the TATA-box and CAAT-box elements, which are essential for recruiting basal transcriptional machinery, defining the transcription start site, and determining promoter efficiency (Porto et al., 2014).

To further investigate the tissue-specific expression of the *rolD-like* gene in *I. batatas*, we performed qPCR analysis across various plant tissues, including leaves at different developmental stages (young, mature, and old). The results revealed a very low expression level in young leaves, which increased as the leaves matured and peaked in old leaves (Fig. 3B). Among all tissues analyzed, the highest expression was observed in storage roots, indicating a potential role in storage-related functions. Moderate expression was detected in the stem, while the apex and fibrous roots exhibited comparatively lower expression levels.

To investigate the potential hormonal influence on *rolD-like* gene we also analyzed its expression in detached *I. batatas* leaves (Fig. 3B). These leaves were treated with 5.71 µM (1 mg/L) IAA, 4.65 µM (1 mg/L) BAP, 50 µM ABA, 50 µM MeJA, and 50 µM SA, with observations taken at both 3 h and 2 days post-treatment. Among the hormones tested, MeJA induced the most pronounced upregulation of the ***rolD-like*** gene. Expression levels peaked 3 h after treatment, showing a **16-fold increase** relative to the untreated control. Although this elevated expression diminished significantly after 2 days, it remained substantially higher than the basal level. In contrast, SA treatment elicited a moderate increase in ***rolD-like*** expression, which was consistent across both time points. Other hormones, including IAA, BAP, and ABA, induced only minor changes in gene expression relative to the control. A slight upregulation was observed at 2 days post-treatment with IAA and at 3 h with ABA and BAP, but these changes were negligible compared to the response elicited by MeJA.

We also assessed the expression levels of the *rolD-like* gene under various stress conditions (Fig. 3B). Heat stress induced the most significant upregulation, with a 35-fold increase in ***rolD-like*** expression observed 3 h post-treatment, which then declined but remained elevated after 48 h. Similarly, high-light stress and dark-induced leaf senescence (DILS) led to notable increases in expression, peaking at approximately 25-fold and 20-fold, respectively. UV stress, measured 1-h post-treatment, also triggered a pronounced upregulation of the ***rolD-like*** gene. Drought stress significantly upregulated ***rolD-like*** expression, with increases observed at both 3 h and 48 h post-treatment. Cold stress led to a moderate upregulation of ***rolD-like*** expression at 3 h, which returned to near-basal levels by 48 h. Salt stress induced by NaCl, as well as osmotic stress caused by mannitol, resulted in minimal expression

changes, with only slight increases recorded. Similarly, paraquat, a reactive oxygen species (ROS) inducer, elicited a limited response, with negligible changes in ***rolD-like*** expression levels.

Finally, we evaluated the expression levels of the *rolD-like* gene in response to treatments with ornithine and proline, two critical metabolites in the OCD pathway (Fig. 3B). Compared to the untreated control, treatment with ornithine resulted in a moderate increase in expression at 3 h, which remained consistent at 48 h. In contrast, proline induced a substantial upregulation of *rolD-like* expression, which increased over time.

3.4. Root-inducing potential of the rolD-like gene

The ability of the *rolD-like* gene to induce hairy root formation was investigated using internodes of *Kalanchoë daigremontiana*. Experimental inoculation with EHA105 carrying the *rolD-like* gene under the control of a double 35 S CaMV promoter did not induce neoplastic growth or root formation (Fig. 4A). Furthermore, co-inoculation of *K. daigremontiana* with *Agrobacterium rhizogenes* K599 and EHA105 carrying the *rolD-like* gene did not enhance root-inducing activity compared to K599 alone (Fig. 4B and C). As expected, the negative control using *A. tumefaciens* EHA105 without a gene insert failed to induce root formation (Fig. 4D). These findings indicate that the *rolD-like* gene, even when driven by a strong promoter, does not independently promote root formation or enhance the root-inducing activity of *A. rhizogenes* K599 in this experimental model.

3.5. Phenotypic analysis of Arabidopsis lines expressing the rolD-like gene

Two transgenic *Arabidopsis thaliana* lines, designated as At-rolD-like 1 and At-rolD-like 2, were generated to express the *rolD-like* gene. These transgenic lines displayed significant phenotypic differences compared to wild-type (WT) plants (Fig. 5A). The most notable morphological difference in the transgenic plants was growth retardation, which became evident during the 3rd to 4th week of cultivation. By the onset of flowering, the height of WT plants was approximately 2–3 times greater than that of the plants expressing the *rolD-like* gene, and this disparity persisted throughout the entire life cycle. Additionally, At-rolD-like plants displayed delayed bolting and reduced inflorescence development compared to WT. Leaf morphology was also significantly affected. The transgenic plants produced smaller leaves compared to WT plants, resulting in a reduced rosette leaf area. Quantitative analysis revealed that the rosette leaf area in WT plants was approximately 1.4 times larger than in the transgenic lines (Fig. 5A).

Transgenic lines also exhibited distinctive alterations in their generative organs. WT plants typically produced inflorescences containing 4 to 10 buds, while transgenic lines consistently formed only 2–3 buds per inflorescence. Remarkably, these buds were larger than those of WT plants and densely covered with trichomes, a feature absent in WT buds (Fig. 5B). Furthermore, the silique of transgenic plants were approximately four times smaller than WT silique, leading to a substantial reduction in seed number per pod. Transgenic plants produced only 1–5 seeds per pod, compared to 20–40 seeds in WT plants (Fig. 5B).

Root architecture was also examined to determine if the *rolD-like* gene influenced root development. Both WT and transgenic plants were grown vertically on half-strength MS agar plates for 10 days. No significant differences in root length, area, or number were observed between the WT and transgenic lines (Fig. 5C).

3.6. The influence of the rolD-like gene on proline production and OCD activity

To evaluate the enzymatic functionality of the *rolD-like* gene in transgenic *Arabidopsis* plants, we conducted a comprehensive chemical analysis. Proline quantification was carried out using hydrophilic interaction chromatography (HILIC) with a silica stationary phase coupled to ESI-MS detection (Fig. 6A). Protonated molecular ions ($[M+H]^+$) at *m/z* 116 were identified as the predominant ions under mild electrospray ionization conditions, confirming the presence of proline (Fig. 6B). The product ion spectra of the precursor $[M+H]^+$ ions revealed a primary fragment ion at *m/z* 70, which corresponds to the loss of formic acid (46 Da), further validating the identification of proline (Fig. 6B). The acquisition of MS/MS spectra was essential to ensure the precise identification of proline in all analyzed samples.

Quantitative analysis using HPLC-MS demonstrated a remarkable increase in proline content in leaves of rolD-like-expressing transgenic plants. These lines showed a 24- and 31-fold elevation in L-proline levels compared to wild-type (WT) plants (Fig. 6C).

In addition to proline quantification, the OCD enzymatic activity of plant extracts was assessed via an *in vitro* assay. The results revealed a substantial increase in NADH production in transgenic lines expressing the *rolD-like* gene, which was absent in WT plants (Fig. 6D).

3.7. Molecular analysis of biological functions of rolD-like gene in transgenic Arabidopsis

To assess the impact of *rolD-like* gene expression in transgenic *Arabidopsis* lines, we first quantified *rolD-like* transcripts using qPCR analysis (Fig. 7). Interestingly, the expression levels differed markedly between the lines, with At-rolD-like2 exhibiting over a threefold higher transcript abundance compared to At-rolD-like1.

The transcriptional changes in defense-related genes were profound. The expression of *PR1* and *PR5* was dramatically elevated, with increases of 1093–1553-fold and 218–317-fold, respectively, relative to WT (Fig. 7). These upregulations correlated with the level of *rolD-like* transgene expression. Additionally, *NPR1*, a central regulator of systemic acquired resistance, exhibited a twofold increase, indicating enhanced activation of defense signaling pathways.

In the abscisic acid (ABA) signaling pathway, expression of the receptor components *PYR* and *PYL* decreased twofold in the transgenic

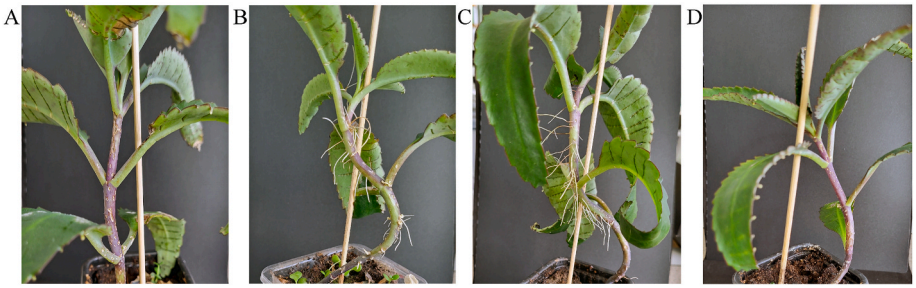

Fig. 4. Effects of *Agrobacterium* strains on root formation in *Kalanchoë daigremontiana*. (A) *A. tumefaciens* EHA105 carrying the *rolD-like* gene under the control of a double 35 S CaMV promoter. (B) Co-inoculation of *A. rhizogenes* K599 with *A. tumefaciens* EHA105 carrying the *rolD-like* gene. (C) Positive control: *A. rhizogenes* K599, showing typical hairy roots. (D) Negative control: *A. tumefaciens* EHA105 without any insert.

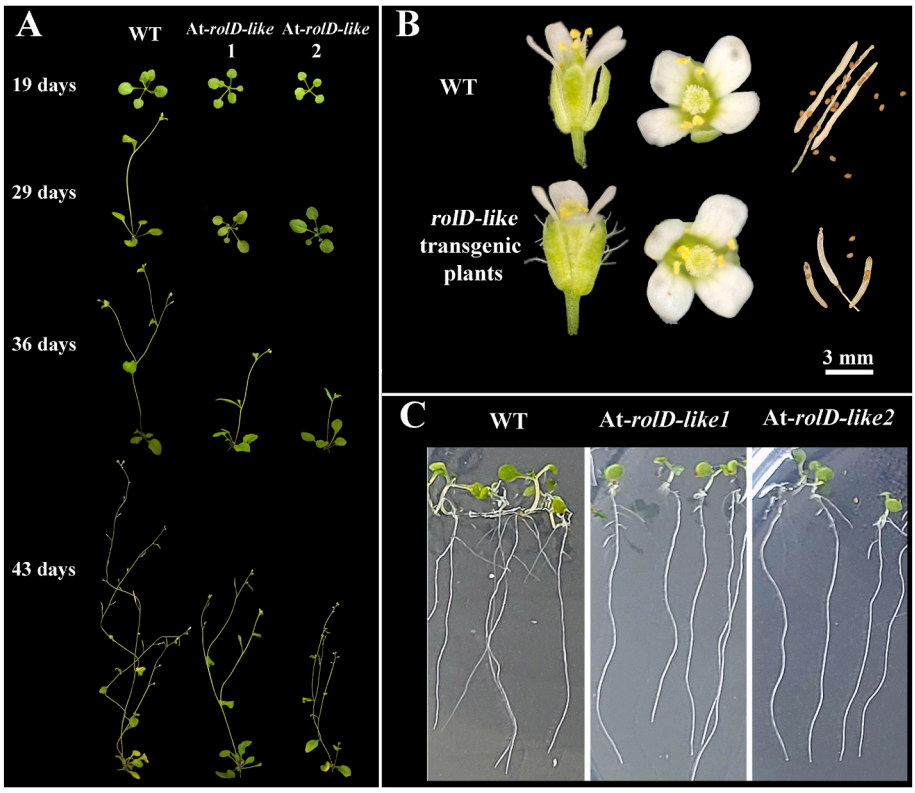

Fig. 5. Phenotypic characterization of *Arabidopsis* lines expressing the *rolD-like* gene. (A) Growth phenotypes of wild-type (WT) and *rolD-like*-expressing *Arabidopsis* lines at different time points (19, 29, 36, and 43 days after planting). (B) Morphological differences in flowering organs and silique of WT and transgenic plants, highlighting reduced seed production and trichome presence in At-rolD-like lines. (C) Root growth analysis of WT and At-rolD-like plants grown vertically on half-strength MS medium for 10 days.

lines (Fig. 7). Similarly, ABA-inducible genes, including *HAI1* phosphatase and *SnRK2s* kinase, showed a 1.5-fold reduction in transcription compared to WT, suggesting reduced ABA sensitivity in the transgenic plants.

Salicylic acid (SA) biosynthesis was examined through two pathways: the isochorismate pathway in chloroplasts and the phenylalanine pathway. Genes involved in the isochorismate pathway (*ICS1*, *PBS3*, and *EPS1*) were upregulated by 2–4-fold in the transgenic lines (Fig. 7). However, *AIM1*, a key enzyme in the phenylalanine pathway, showed a 1–2-fold reduction in transcription, indicating a shift toward the chloroplast-localized SA biosynthesis pathway.

Jasmonic acid (JA) biosynthesis exhibited substantial modulation. The *LOX2* gene, responsible for the initial step of JA synthesis, was upregulated 6.7–9-fold in the transgenic lines compared to WT (Fig. 7). The downstream *OPR3* gene involved in peroxisomal JA biosynthesis was upregulated 3.9- and 2.8-fold in At-rolD-like1 and At-rolD-like2, respectively, while *OPR2* expression remained unchanged. Intriguingly, the expression of JA signaling genes *JAR1* and *JMT* was reduced by half in the transgenic lines, indicating potential modulation of downstream JA pathways.

Minimal alterations were observed in genes associated with reactive oxygen species (ROS) detoxification. While ascorbate peroxidases (*Apx1–3*) were not activated, the transcription of *CSD2* (superoxide dismutase 2) and *Cat1* (catalase 1) was reduced in the transgenic lines compared to WT plants (Fig. 7).

3.8. Modulation of flavonoid biosynthesis by the rolD-like gene

To evaluate the impact of the *rolD-like* gene on secondary metabolism, we quantified the levels of flavonol glycosides in transgenic *Arabidopsis* plants and compared them to WT plants. The analysis revealed the pronounced increase in the total flavonol glycoside content, which was approximately 3-fold higher in At-rolD-like1 and 4-fold higher in At-rolD-like2 compared to WT plants (Table 1).

Among the flavonol glycosides analyzed, the levels of kaempferol hexose-dideoxyhexose were notably elevated in both transgenic lines, with At-rolD-like2 exhibiting the highest concentration (Table 1). Similarly, quercetin hexose-dideoxyhexose, kaempferol hexose-deoxyhexose, and isorhamnetin hexose-deoxyhexose showed increased accumulation in the transgenic lines, albeit to a lesser extent. In contrast, the WT plants maintained relatively low levels of these compounds.

To further investigate the molecular mechanisms underlying the increased accumulation of flavonol glycosides in the *rolD-like*-expressing transgenic *Arabidopsis* plants, we analyzed the expression levels of key genes involved in the flavonoid biosynthetic pathway. Quantitative PCR revealed significant changes in the transcription of multiple pathway-related genes in both At-rolD-like1 and At-rolD-like2 lines compared to the WT plants. The phenylpropanoid pathway genes *PAL*, *C4H*, and 4 C L, which are responsible for the early steps of flavonoid biosynthesis, were significantly upregulated in the transgenic lines (Fig. 8). The expression of *PAL* showed the highest increase, with transcript levels elevated approximately 10-fold compared to WT plants. Similarly, *C4H* and 4 C L were upregulated by 8–10 times. In contrast, the expression of *CHS* (chalcone synthase), which catalyzes the first committed step in flavonoid biosynthesis, was markedly reduced in both transgenic lines, with transcript levels approximately fivefold lower than in WT plants (Fig. 8). The downstream genes *F3H*, *F3′H*, and *FLS*, involved in the conversion of flavanones to flavonols, showed differential regulation. *F3H* and *FLS* were significantly upregulated, with transcript levels approximately 6-fold and 4-fold higher, respectively, in the transgenic lines than in WT plants (Fig. 8). However, the expression of *F3′H* remained largely unchanged across all lines, indicating that the flux toward specific flavonoid subgroups might be selectively regulated.

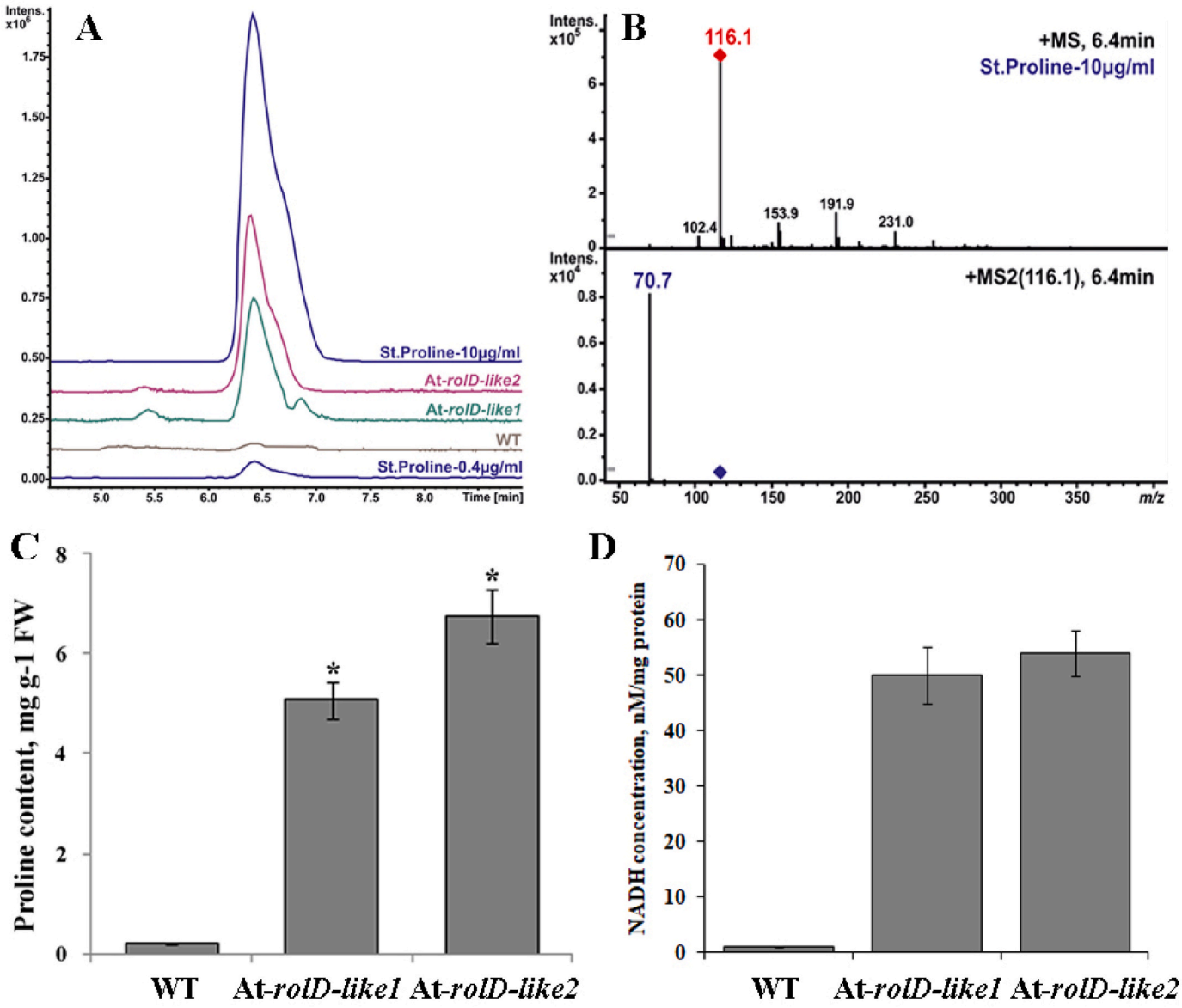

Fig. 6. The impact of *rolD-like* gene expression on proline production and enzymatic activity in transgenic *Arabidopsis*. (A) Targeted LC-MS analysis of proline in plant extracts, showing extracted ion chromatograms at *m/z* 116 ± 1 for proline ($[M+H]^+$). (B) MS/MS spectra of the proline standard solution. (C) Proline content in the leaves of wild-type (WT) and *rolD-like*-expressing *Arabidopsis* lines. (D) NADH production during the *in vitro* enzymatic conversion of L-ornithine to L-proline in WT and *rolD-like*-expressing *A. thaliana* plant extracts. NADH accumulation was quantified spectrophotometrically at 340 nm. The data are presented as means ± SE based on three biological replicates, each consisting of 10 plants. Statistical significance was assessed using the LSD test at $P < 0.05$, with values sharing the same letter indicating no significant difference.

4. Discussion

This study identifies and characterizes a novel *rolD-like* gene naturally integrated into the cT-DNA2 region of the sweet potato (*Ipomoea batatas*) genome. While natural transgenes are widely observed in plant genomes (Matveeva and Otten, 2019), homologs of the *Agrobacterium*-derived *rolD* gene remain notably rare. The *rolD* gene was identified within the so-called TD insertion in the genome of the ancestral tobacco species *N. tomentosiformis*, closely resembling the TL-DNA region from *A. rhizogenes* A4 (Chen et al., 2014). Additionally, PCR-based studies detected a similar TD region in cT-DNAs in *N. kawakamii* and *N. tomentosa*, although it remains unclear whether this region includes the *rolD* gene (Chen et al., 2014). The rarity of *rolD* homologs in plant genomes likely stems from its exclusive association with agropine-type Ri plasmids, making transformation by *rolD* less frequent than by *rolB* and *rolC* genes, which are widely distributed across *Agrobacterium* strains.

Here, we demonstrate that the ***rolD-like*** gene encodes a functional ornithine cyclodeaminase (OCD) protein, catalyzing the conversion of L-ornithine to L-proline with NADH production as a byproduct. This function mirrors that of the *Agrobacterium rolD* gene, the only *rol* gene with a well-established role, which is localized in the cytoplasm and is pivotal in proline biosynthesis (Trovato et al., 2001). Notably, the RolD-like protein exhibited slightly different kinetic behavior compared to RolD, possibly due to variations in substrate affinity, catalytic efficiency, or cofactor interactions. Despite these differences, the RolD-like protein showed robust OCD activity both *in vitro* and *in vivo*, highlighting its functional conservation and potential biological relevance. Interestingly, OCD has been identified only in certain prokaryotes, including *Agrobacterium*, *Sinorhizobium*, and *Rhodobacterium*, as well as extremophile archaea (Trovato et al., 2018). In *A. tumefaciens*, a similar enzyme is involved in the catabolism of opines synthesized in transformed plant

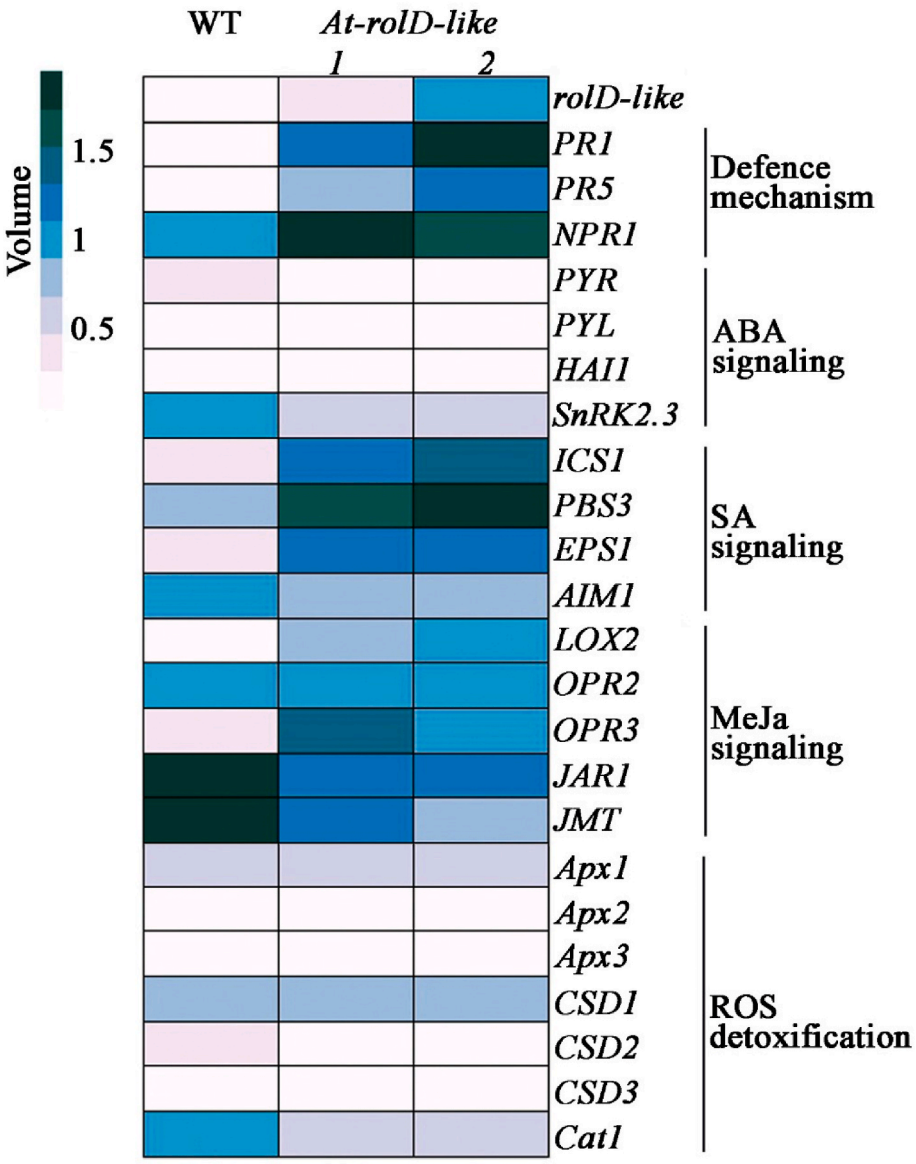

Fig. 7. Expression analysis of genes involved in the defense system, hormonal regulation, and antioxidant pathways in wild-type (WT) plants and *rolD-like*-expressing *A. thaliana* lines. The data are presented as means ± SE based on three biological replicates, each consisting of 10 plants.

Table 1
Effect of the *rolD-like* gene on flavonol glycosides content (μmol/g DW) in transgenic *Arabidopsis* lines.

	WT	*At-rolD-like 1*	*At-rolD-like 2*
Quercetin hexose dideoxyhexose	n.d.	0.103 ± 0.034*	0.090 ± 0.002*
Kaempferol hexose dideoxyhexose	0.116 ± 0.016	0.923 ± 0.102*	1.085 ± 0.064*
Quercetin hexose deoxyhexose	n.d.	0.159 ± 0.004*	0.147 ± 0.009*
Kaempferol hexose deoxyhexose	0.044 ± 0.001	0.408 ± 0.020*	0.538 ± 0.350*
Isorhametin hexose deoxyhexose	n.d.	0.201 ± 0.019*	0.264 ± 0.014*
Kaempferol dideoxyhexose	n.d.	1.856 ± 0.235*	2.360 ± 0.150*
Sum of flavonol glycosides	0.159 ± 0.016	3.655 ± 0.260*	4.483 ± 0.270*

Data represent mean ± SE of three biological replicates. Asterisks indicate statistically significant differences relative to WT (*$p \leq 0.05$), Student's t-test. n.d. – not detected.

cells. However, this gene, although present on the Ti plasmid, lies outside the T-DNA region and is therefore not transferred to plant genomes during transformation (Sans et al., 1988). In contrast, an OCD-like protein in *Arabidopsis thaliana* showed no activity toward ornithine as a substrate and, consequently, did not influence proline accumulation (Sharma et al., 2013).

The expression patterns of *rolD* and *rolD-like* genes exhibit notable differences. The *rolD* gene has been reported to show the highest expression in stems, with lower levels in roots and leaves (Trovato et al., 1997). Conversely, other studies have indicated that *rolD* transcripts are predominantly localized in root tissues (Leach and Aoyagi, 1991). In contrast, the *rolD-like* gene exhibits its highest expression in storage roots, suggesting a functional role in storage metabolism. Its expression in stems and leaves was moderate, with the lowest levels observed in roots. Although *rolD* may enhance hairy root growth, likely by facilitating proline provision, this gene is neither strictly necessary for their induction nor capable of initiating them independently (Trovato et al., 2001). Similarly, the *rolD-like* gene did not induce root formation in *Kalanchoë daigremontiana* internodes, even under the transcriptional control of the strong double 35 S CaMV promoter.

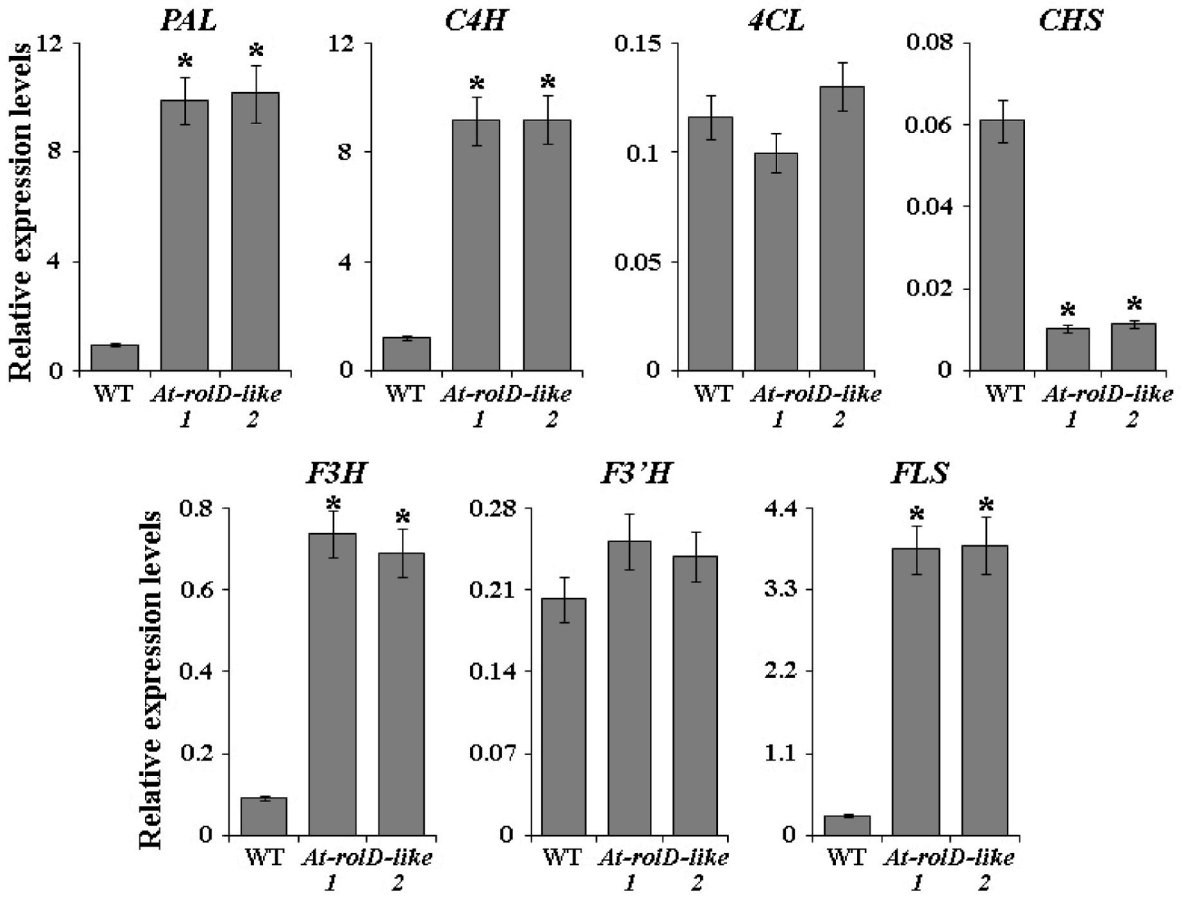

Fig. 8. Expression analysis of key flavonoid biosynthetic genes in WT and *rolD-like*-expressing *Arabidopsis* lines. Data represent mean ± SE of three biological replicates. Asterisks indicate statistically significant differences relative to WT (*$p \leq 0.05$), Student's t-test.

Hormonal regulation of *rolD-like* expression further underscores its functional divergence from *rolD*. While *rolD* is auxin-inducible through a Dof-binding motif (Mauro et al., 2002), *rolD-like* exhibited no significant response to IAA, BAP, or ABA. Instead, it showed strong responsiveness to MeJA and moderate regulation by SA, implicating its involvement in stress hormone signaling pathways. Furthermore, the *rolD-like* gene was highly upregulated by abiotic stressors, including heat, cold, drought, high light, and UV stress. This expression pattern aligns with cis-regulatory motifs identified in its promoter, such as DRE1, LTR, CGTCA, P-box, G-box, and Box-4, which are known to mediate responses to stress and hormonal signals (Yamaguchi-Shinozaki and Shinozaki, 2005; Niu et al., 2018; Rouster et al., 1997; Ma et al., 2013). These findings highlight the potential role of *rolD-like* in sweet potato's stress adaptation.

Transgenic *Arabidopsis* plants expressing *rolD-like* exhibited significant morphological changes, correlating with transgene expression levels. One prominent phenotype was significant growth inhibition, consistent with findings in *rolD*-transgenic *Arabidopsis* plants (Falasca et al., 2010). Furthermore, *rolD* expression in carrot caused severe dwarfism, wrinkled leaves, and curved petioles (Limami et al., 1998). However, no such growth inhibition was observed in *rolD*-expressing tobacco and tomato (Bettini et al., 2003; Mauro et al., 1996). Interestingly, while *rolD* accelerates flowering in *Arabidopsis* (Falasca et al., 2010) this effect was absent in At-rolD-like lines. The contrasting phenotypes between *rolD* and *rolD-like* may reflect functional differences in their interactions with hormonal pathways or their promoter-driven expression patterns (native *rolD* versus viral 35 S CaMV). Reduced leaf size in *rolD-like* transgenic plants may be attributed to elevated proline levels, consistent with findings in *Medicago sativa*, where high proline concentrations inhibited leaf and shoot growth (Srhiouar et al., 2022). In our study, *rolD-like*-expressing transgenic *Arabidopsis* plants showed a striking increase in proline levels, reaching up to 31-fold higher than in wild-type plants.

Proline is a well-established osmoprotectant critical for plant stress tolerance, facilitating osmotic adjustment, scavenging reactive oxygen species (ROS), and stabilizing cellular membranes (Hayat et al., 2012). The upregulation of stress-responsive genes, such as *PR-1* and *PR-5*, further supports the role of the *rolD-like* gene in enhancing stress adaptation. Notably, increased *PR-1* production has also been reported in *rolD*-expressing plants as part of their defense response (Bettini et al., 2003). Similarly, the elevated expression of SA biosynthetic genes (*ICS1*, *PBS3*, and *EPS1*) and JA biosynthetic genes (*LOX2* and *OPR3*) indicates the integration of *rolD-like* activity into key hormonal signaling pathways involved in stress responses. In contrast, *rolD-like* unexpectedly reduced the expression of antioxidant genes such as *CSD2* and *Cat1*. This downregulation is surprising, as it differs from the typical upregulation of these genes observed in *rol*-expressing plant cells, where enhanced ROS scavenging potential is a key mechanism for maintaining cellular homeostasis under stress (Favero et al., 2021; Shvets et al., 2024). It is plausible that in *rolD-like*-transgenic lines, antioxidant protection is compensated by flavonoids, whose content significantly increased. Flavonoids are known to play a critical role in mitigating oxidative damage, and their overaccumulation in *A. thaliana* has been shown to significantly enhance oxidative and drought tolerance, as evidenced by reduced ROS levels (Nakabayashi et al., 2014).

In summary, this study establishes the *rolD-like* gene encoded in the cellular *Ib*T-DNA2 of a naturally transgenic sweet potato plant as a potential player in plant stress adaptation and secondary metabolism. Its

integration into the sweet potato genome exemplifies the potential of horizontal gene transfer to enhance plant resilience and suggests that such natural transgenes may have conferred selective advantages during evolution. From a biotechnological perspective, the *rolD-like* gene offers new opportunities for crop improvement. However, the trade-offs between stress tolerance and reproductive fitness remain a critical consideration for its practical application. While our study demonstrates its role in stress adaptation, further research is needed to evaluate its effects on reproductive traits in sweet potato, including flowering, seed set, and tuber yield under variable environmental conditions.

Declaration of competing interest

The authors declare that they have no known competing financial interests or personal relationships that could have appeared to influence the work reported in this paper.

Acknowledgments

Financial support was provided by the Russian Science Foundation, Grant no. 23-74-01082 (Yugay Y.A.). The experiments described in this work were performed using equipment from the Instrumental Centre for Biotechnology and Gene Engineering at the Federal Scientific Centre of East Asia Terrestrial Biodiversity of the Far East Branch of the Russian Academy of Sciences.

Appendix A. Supplementary data

Supplementary data to this article can be found online at https://doi.org/10.1016/j.plaphy.2025.109875.

Data availability

Data will be made available on request.

References

Bettini, P., Michelotti, S., Bindi, D., Giannini, R., Capuana, M., Buiatti, M., 2003. Pleiotropic effect of the insertion of the *Agrobacterium rhizogenes rolD* gene in tomato (*Lycopersicon esculentum* Mill.). Theor. Appl. Genet. 107, 831–836.

Chen, K., Dorlhac, B.F., Szegedi, E., Otten, L., 2014. Deep sequencing of the ancestral tobacco species *Nicotiana tomentosiformis* reveals multiple T-DNA inserts and a complex evolutionary history of natural transformation in the genus *Nicotiana*. Plant J. 80, 669–682.

Falasca, G., Altamura, M.M., D'Angeli, S., Zaghi, D., Costantino, P., Mauro, M.L., 2010. The *rolD* oncogene promotes axillary bud and adventitious root meristems in *Arabidopsis*. Plant Physiol. Biochem. 48, 797–804.

Favero, B.T., Tan, Y., Lin, Y., Hansen, H.B., Shadmani, N., Xu, J., He, J., Müller, R., Almeida, A., Lütken, H., 2021. Transgenic *Kalanchoë blossfeldiana*, containing individual rol genes and open reading frames under 35S promoter, exhibit compact habit, reduced plant growth, and altered ethylene tolerance in flowers. Front. Plant Sci. 12, 672023.

Geertz-Hansen, H.M., Blom, N., Feist, A.M., Brunak, S., Petersen, T.N., 2014. Cofactory: sequence-based prediction of cofactor specificity of Rossmann folds. Proteins: Struct., Funct., Bioinf. 82, 1819–1828.

Goodman, J.L., Wang, S., Alam, S., Ruzicka, F.J., Frey, P.A., Wedekind, J.E., 2004. Ornithine cyclodeaminase: structure, mechanism of action, and implications for the μ-crystallin family. Biochemistry 43, 13883–13891.

Hayat, S., Hayat, Q., Alyemeni, M.N., Wani, A.S., Pichtel, J., Ahmad, A., 2012. Role of proline under changing environments: a review. Plant Signal. Behav. 7, 1456–1466.

Imbo, M.C., Budambula, N.L.M., Mweu, C.M., Muli, J.K., Anami, S.E., 2016. Genetic transformation of sweet potato for improved tolerance to stress: a review. Adv. Life Sci. Technol. 49, 67–76.

Kays, S., 2005. Sweetpotato production worldwide: assessment, trends and the future. Acta Hortic. 670, 19–25.

Kelley, L., Mezulis, S., Yates, C., Wass, M.N., Sternberg, M.J.E., 2015. The Phyre2 web portal for protein modeling, prediction, and analysis. Nat. Protoc. 10, 845–858.

Kwak, S.S., 2019. Biotechnology of the sweetpotato: ensuring global food and nutrition security in the face of climate change. Plant Cell Rep. 38, 1361–1363.

Kyndt, T., Quispe, D., Zhai, H., Jarret, R., Ghislain, M., Liu, Q., Gheysen, G., Kreuze, J.F., 2015. The genome of cultivated sweet potato contains Agrobacterium T-DNAs with expressed genes: an example of a naturally transgenic food crop. Proc. Natl. Acad. Sci. 112, 5844–5849.

Laurie, S.M., Bairu, M.W., Laurie, R.N., 2022. Analysis of the nutritional composition and drought tolerance traits of sweet potato: selection criteria for breeding lines. Plants 11, 1804. https://doi.org/10.3390/plants11141804.

Leach, F., Aoyagi, K., 1991. Promoter analysis of the highly expressed rolC and rolD root-inducing genes of Agrobacterium rhizogenes: enhancer and tissue-specific DNA determinants are dissociated. Plant Sci. 79, 69–76.

Lescot, M., Déhais, P., Thijs, G., Marchal, K., Moreau, Y., Van de Peer, Y., Rouzé, P., Rombauts, S., 2002. PlantCARE, a database of plant cis-acting regulatory elements and a portal to tools for *in silico* analysis of promoter sequences. Nucleic Acids Res. 30, 325–327.

Limami, M.A., Sun, L.-Y., Douat, C., Helgeson, J., Tepfer, D., 1998. Natural genetic transformation by *Agrobacterium rhizogenes*. Plant Physiol 118, 543–550.

Ma, S., Shah, S., Bohnert, H.J., Snyder, M., Dinesh-Kumar, S.P., 2013. Incorporating motif analysis into gene co-expression network reveals novel modular expression pattern and new signaling pathways. PLoS Genet. 9, e1003840.

Mahesh, M.V.N.U., Faidh, M.A., Chadha, A., 2022. The ornithine cyclodeaminase/μ-crystallin superfamily of proteins: a novel family of oxidoreductases for the biocatalytic synthesis of chiral amines. Curr. Res. Biotechnol. 4, 402–419.

Matveeva, T.V., Otten, L., 2019. Widespread occurrence of natural genetic transformation of plants by *Agrobacterium*. Plant Mol. Biol. 101, 415–437.

Mauro, M.L., Trovato, M., De Paolis, A., Gallelli, A., Costantino, P., Altamura, M.M., 1996. The plant oncogene *rolD* stimulates flowering in transgenic tobacco plants. Dev. Biol. 180, 693–700.

Mauro, M.L., De Lorenzo, G., Costantino, P., Bellincampi, D., 2002. Oligogalacturonides inhibit the induction of late but not of early auxin-responsive genes in tobacco. Planta 215, 494–501.

Motsa, N.M., Modi, A.T., Mabhaudhi, T., 2015. Sweet potato (Ipomoea batatas L.) as a drought tolerant and food security crop. South Afr. J. Sci. 111, 8.

Mukhopadhyay, S.K., Chattopadhyay, A., Chakraborty, I., Bhattacharya, I., 2011. Crops that feed the world 5. Sweetpotato. Sweetpotatoes for income and food security. Food Secur. 3, 283–305.

Nakabayashi, R., Yonekura-Sakakibara, K., Urano, K., Suzuki, M., Yamada, Y., Nishizawa, T., Matsuda, F., Kojima, M., Sakakibara, H., Shinozaki, K., Michael, A.J., Tohge, T., Yamazaki, M., Saito, K., 2014. Enhancement of oxidative and drought tolerance in *Arabidopsis* by overaccumulation of antioxidant flavonoids. Plant J. 77, 367–379.

Niu, G.-L., Gou, W., Han, X.-L., Qin, C., Zhang, L.-X., Abomohra, A.E.-F., Ashraf, M., 2018. Cloning and functional analysis of phosphoethanolamine methyltransferase promoter from maize (*Zea mays* L.). Int. J. Mol. Sci. 19, 191.

Porto, M.S., Pinheiro, M.P.N., Batista, V.G.L., Santos, R.C., Filho, P.d.A.M., Lima, L.M., 2014. Plant promoters: an approach of structure and function. Mol. Biotechnol. 56, 38–49.

Quispe-Huamanquispe, D.G., Gheysen, G., Yang, J., Jarret, R., Rossel, G., Kreuze, J.F., 2019. The horizontal gene transfer of *Agrobacterium* T-DNAs into the series Batatas (Genus *Ipomoea*) genome is not confined to hexaploid sweet potato. Sci. Rep. 9, 12584.

Rodriguez-Bonilla, L., Cuevas, H.E., Montero-Rojas, M., Bird-Pico, F., Luciano-Rosario, D., Siritunga, D., 2014. Assessment of genetic diversity of sweet potato in Puerto Rico. PLoS One 9, e116184.

Rouster, J., Leah, R., Mundy, J., Cameron-Mills, V., 1997. Identification of a methyl jasmonate-responsive region in the promoter of a lipoxygenase 1 gene expressed in barley grain. Plant J. 11, 513–523.

Sans, N., Schindler, V., Schröder, J., 1988. Ornithine cyclodeaminase from Ti plasmid C58: DNA sequence, enzyme properties and regulation activity by arginine. Eur. J. Biochem. 173, 123–130.

Sapakhova, Z., Raissova, N., Daurov, D., Zhapar, K., Daurova, A., Zhigailov, A., Zhambakin, K., Shamekova, M., 2023. Sweet potato as a key crop for food security under the conditions of global climate change: a review. Plants 12, 2516.

Schmidt, R., Schippers, J.H.M., Mieulet, D., Watanabe, M., Hoefgenb, R., Guiderdonic, E., Mueller-Roebera, B., 2014. SALT-RESPONSIVE ERF1 is a negative regulator of grain filling and gibberellin-mediated seedling establishment in rice. Mol. Plant 7, 404–421.

Sharma, S., Shinde, S., Verslues, P.E., 2013. Functional characterization of an ornithine cyclodeaminase-like protein of *Arabidopsis thaliana*. BMC Plant Biol. 13, 182.

Shkryl, Y., Yugay, Y., Avramenko, T., Grigorchuk, V., Gorpenchenko, T., Grischenko, O., Bulgakov, V., 2021. CRISPR/Cas9-Mediated knockout of *HOS1* reveals its role in the regulation of secondary metabolism in *Arabidopsis thaliana*. Plants 10, 104.

Shkryl, Y.N., Vasyutkina, E.A., Gorpenchenko, T.V., Mironova, A.A., Rusapetova, T.V., Velansky, P.V., Bulgakov, V.P., Yugay, Y.A., 2024. Salicylic acid and jasmonic acid biosynthetic pathways are simultaneously activated in transgenic *Arabidopsis expressing* the *rolB/C* gene from *Ipomoea batatas*. Plant Physiol. Biochem. 208, 108521.

Shvets, D.Yu, Berezhneva, Z.A., Musin, KhG., Kuluev, B.R., 2024. Effect of *rol* genes of the A4, 15834, and K599 strains of *Agrobacterium rhizogenes* on root growth and states of the antioxidant systems of transgenic tobacco plants subjected to abiotic stress. Russ. J. Plant Physiol. 71, 165.

Srhiouar, N., Ferioun, M., Bouhraoua, S., Hammani, K., Louahlia, S., 2022. Impact of severe salt stress on morphological, physiological, and biochemical parameters in alfalfa (*Medicago sativa* L.). Environ. Sci. Proc. 16, 27.

Szabados, L., Savouré, A., 2010. Proline: a multifunctional amino acid. Trends Plant Sci. 15, 89–97.

Trovato, M., Mauro, M.L., Costantino, P., Altamura, M.M., 1997. The *rolD* gene from *Agrobacterium rhizogenes* is developmentally regulated in transgenic tobacco. Protoplasma 197, 111–120.

Trovato, M., Maras, B., Linhares, F., Costantino, P., 2001. The plant oncogene *rolD* encodes a functional ornithine cyclodeaminase. Proc. Natl. Acad. Sci. 98, 13449–13453.

Trovato, M., Mattioli, R., Costantino, P., 2018. From *A. rhizogenes* RolD to plant P5CS: exploiting proline to control plant development. Plants 7, 108.

Vasyutkina, E.A., Yugay, Y.A., Grigorchuk, V.P., Grishchenko, O.V., Sorokina, M.R., Yaroshenko, Y.L., Kudinova, O.D., Stepochkina, V.D., Bulgakov, V.P., Shkryl, Y.N., 2022. Effect of stress signals and ib-rolB/C overexpression on secondary metabolite biosynthesis in cell cultures of Ipomoea batatas. Int. J. Mol. Sci. 23, 15100.

Yamaguchi-Shinozaki, K., Shinozaki, K., 2005. Organization of cis-acting regulatory elements in osmotic- and cold-stress-responsive promoters. Trends Plant Sci. 10, 88–94.

Yan, H., Ma, M., Ahmad, M.Q., Arisha, M.H., Tang, W., Li, C., Zhang, Y., Kou, M., Wang, X., Gao, R., Song, W., Li, Z., Li, Q., 2022. High-density single nucleotide polymorphisms genetic map construction and quantitative trait locus mapping of color-related traits of purple sweet potato [*Ipomoea batatas* (L.) lam.]. Front. Plant Sci. 12, 797041.

Yin, G., Xu, H., Xiao, S., Qin, Y., Li, Y., Yan, Y., Hu, Y., 2013. The large soybean (*Glycine max*) WRKY TF family expanded by segmental duplication events and subsequent divergent selection among subgroups. BMC Plant Biol. 13, 148.